DOI: 10.1002/ejic.200900847

Control of Exchange Interactions in Trinuclear Complexes Based on Orthogonal Magnetic Orbitals

Birgit Weber,*[a] Jaroslava Obel,[a] Lucia R. Lorenz,[a] Wolfgang Bauer,[a] Luca Carrella,[b] and Eva Rentschler[b]

Keywords: Magnetic properties / Schiff bases / Copper / Vanadium / N,O ligands

The reaction of copper(II) acetate with the tetradentate Schiff base like ligand H_4L {(*E*,*E*)-[{diethyl 2,2′-[4,5-dihydroxy-1,2-phenylenebis(iminomethylidyne)]bis(3-oxobutanoate)}] leads to the formation of the square planar N_2O_2 coordinated complex $[H_2CuL]$. Reaction of two equivalents of this complex with copper(II) acetylacetonato or vanadyl(IV) acetylacetonato yields the trinuclear complexes $[V(O)Cu_2L_2][N(n\text{Bu})_4]_2\cdot 2\text{MeOH}$ (**1**) and $[Cu_3L_2][N(n\text{Bu})_4]_2\cdot 2\text{DMF}$ (**2**). Both complexes were characterised by using magnetic measurements and X-ray crystallography. Special attention was given to the spin-exchange coupling through the bridging phenylene ring. The principle of strict orthogonality of the magnetic orbitals can be applied to explain the results of the susceptibility measurements.

Introduction

The purposeful design of oligonuclear compounds with spins that are aligned in a parallel manner that exhibit spontaneous magnetisation below a critical temperature is one of the major goals of an inorganic chemist working in the field of molecular magnetism, as numerous applications can be envisioned for such materials.[1] Several strategies can be employed to obtain molecules with ferromagnetic exchange interactions. Next to the use of orthogonal magnetic orbitals,[2] the double exchange mechanism[3] and the spin-polarisation mechanism[4] are known to stabilise a high-spin (HS) ground-state. In our research group we investigate the structure and magnetic properties of complexes with Schiff base like N_2O_2 coordinating ligands.[5] Octahedral iron(II) complexes of this ligand type are highly suitable for the observation of thermally induced spin transitions.[6] In contrast, for pure HS iron(II) complexes of this ligand type a spontaneous magnetisation at low temperatures was observed, which could be explained with a spin canting mechanism mediated over hydrogen bonds.[7] Recently, we demonstrated that hydrogen bonds not only play a crucial role for long-range magnetic ordering,[7] but they can also be responsible for strong cooperative interactions in spin-crossover complexes.[8]As a consequence of this finding, we designed a new ligand H_4L based on 4,5-diaminocatechol with two additional hydroxy groups on the phenyl ring that can act as H-bond donors/acceptors.[9] First investigations on the structure and magnetic properties of its iron(II) complexes showed that thermal spin transitions are observed for the octahedral complexes[10] and the number of intermolecular H-bonds increased relative to the number in the original complexes.[9] Rosa and coworkers reported for similar Schiff base ligands the synthesis of trinuclear NiV(O)Ni complexes by deprotonation of the hydroxy groups on the phenyl ring of the monomer nickel(II) complexes.[11] Inspired by this idea, we synthesised the trinuclear complexes $[V(O)Cu_2L_2]\{N(n\text{Bu})_4\}_2\cdot 2\text{MeOH}$ (**1**) and $[Cu_3L_2]\{N(n\text{Bu})_4\}_2\cdot 2\text{DMF}$ (**2**) and investigated their magnetic properties. Some similarities can be found between the bridging motive of the complexes discussed in this paper and the dinuclear complexes $CuVO(fsa)_2en\cdot CH_3OH$ and $Cu_2(fsa)_2en\cdot CH_3OH$ [with $H_4(fsa)_2en$ = *N*,*N*′-(2-hydroxy-3-carboxybenzilidene)ethylenediamine] described by O. Kahn et al. − one of the textbook examples for strict orthogonality of magnetic orbitals.[12] A prediction of the magnetic properties should thus be possible, even though the effects can be expected to be significantly smaller due to the more extended exchange pathway.

Results and Discussion

Synthesis and General Characterisation

In Scheme 1, the general procedure for the synthesis of the mononuclear copper complex $[H_2CuL]$ and trinuclear complexes **1** $\{[V(O)Cu_2L_2](N n\text{Bu}_4)_2\cdot 2\text{MeOH}\}$ and **2** $\{[Cu_3L_2](N n\text{Bu}_4)_2\cdot 2\text{DMF}\}$ is given. The mononuclear cop-

[a] Center for Integrated Protein Science Munich at the Department Chemie und Biochemie, Ludwig-Maximilians-Universität München,
Butenandtstr. 5-13 (Haus F), 81377 München, Germany
Fax: +49-89-2180-77407
E-mail: bwmch@cup.uni-muenchen.de
[b] Institute of Inorganic and Analytical Chemistry, Johannes Gutenberg Universität Mainz,
55099 Mainz, Germany

per complex was obtained by the reaction of the free H_4L ligand with a stoichiometric amount of copper(II) acetate monohydrate in methanol. Reaction of two equivalents of this complex with copper(II) acetylacetonato or vanadyl(IV) acetylacetonato in the presence of tetrabutylammonium hydroxide (TBAH) led to the formation of the trinuclear complexes $[V(O)Cu_2L_2]\{N(n-Bu)_4\}_2 \cdot 2MeOH$ (**1**) and $[Cu_3L_2]\{N(n-Bu)_4\}_2 \cdot 2DMF$ (**2**). The complexes were fully characterised by elemental analysis, IR spectroscopy and mass spectrometry, as well as temperature-dependent magnetic susceptibility measurements.

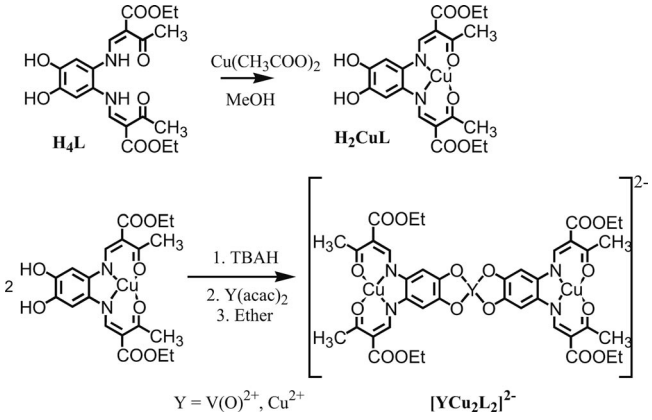

Scheme 1. General procedure for the synthesis of the mononuclear and trinuclear complexes with the used abbreviations.

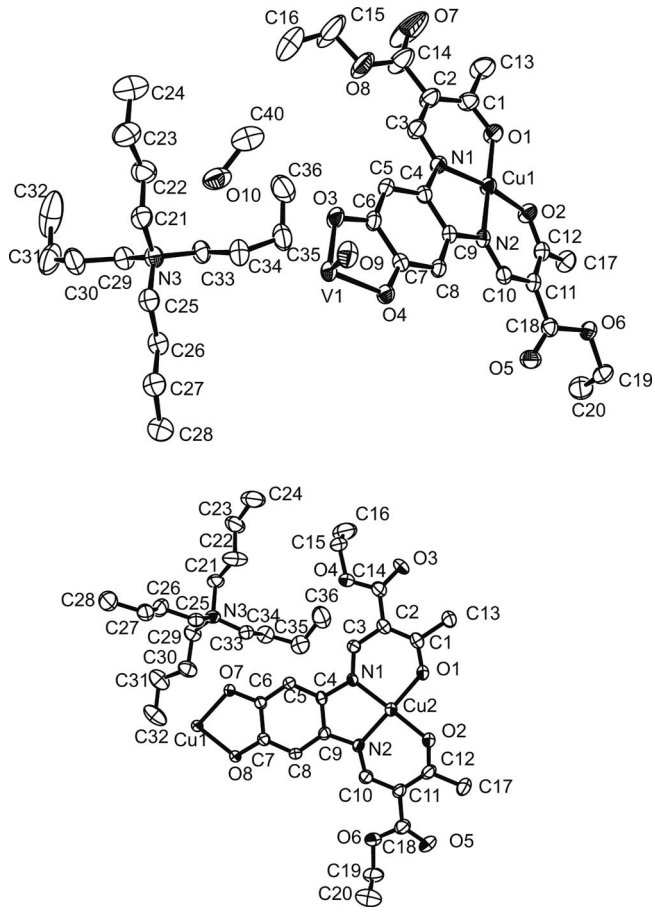

Figure 1. ORTEP drawing of the asymmetric unit of **1** and **2** with the atom numbering scheme. Hydrogen atoms and the DMF molecule in the case of **2** are omitted for clarity. Thermal ellipsoids are shown at the 50% probability level.

Description of the X-ray Structures

Crystals suitable for X-ray structure analysis were obtained for the two trinuclear complexes. The crystallographic data are summarised in Table 4. In Figure 1 an ORTEP drawing of the asymmetric units of the two complexes is displayed. Selected bond lengths and angles within the first coordination sphere are summarised in Table 1. In Figure 2, top and side views of the trinuclear complexes are given.

The outer copper atom is located in the plane of the Schiff base like ligand with a square planar N_2O_2 coordination sphere in both complexes. The Cu–N bond lengths are with an average of 1.92 Å slightly longer than the average Cu–O bond lengths (1.91 Å). The central copper atom in **2** is located in a square planar O_4 coordination sphere with the average Cu–O bond lengths being slightly longer than those for the outer copper centre (1.92 Å). As a consequence, the trinuclear complex is ideally planar with a Cu–Cu–Cu angle of 180°. In contrast to this, the central vanadyl ion is located in a square pyramidal O_5 coordination sphere. The V–O distance to the axial oxygen atom is 1.61 Å, which is significantly shorter than the average distance to the equatorial coordinating oxygen atoms (1.96 Å), in agreement with its double-bond character. Compound **1** assumes a bent structure with a Cu–V–Cu angle of 139°. The intermolecular Cu–Cu and Cu–V distances are 7.70 and 7.78 Å for **2** and **1**, respectively, which are the same order of magnitude, and the Cu–Cu distances are slightly shorter.

In Figures 3 and 4, the packing of the molecules in the crystal is displayed. In the crystal packing the complex molecules form layers with the counterions and additional solvent molecules (MeOH in the case of **1** and DMF in the case of **2**) between the single layers. A hydrogen bond is formed between the complex molecule and the solvent methanol in the case of **1** (Table 2). For **2**, no intermo-

Table 1. Selected bond lengths [Å] and angles [°] within the first coordination spheres of the trinuclear complexes discussed in this work.

	$Cu–N_{eq}$	$Cu–O_{eq}$	Y–O	V=O/V–O_4	O1–Cu–O2	$Cu–N_2O_2$
1	1.921(2)	1.912(2)	1.948(2)	1.612(2)	90.71(7)	0.065
	1.921(2)	1.913(2)	1.971(2)	0.598		
2	1.910(2)	1.908(2)	1.913(2)		88.62(9)	0.038
	1.926(2)	1.910(2)	1.932(2)			

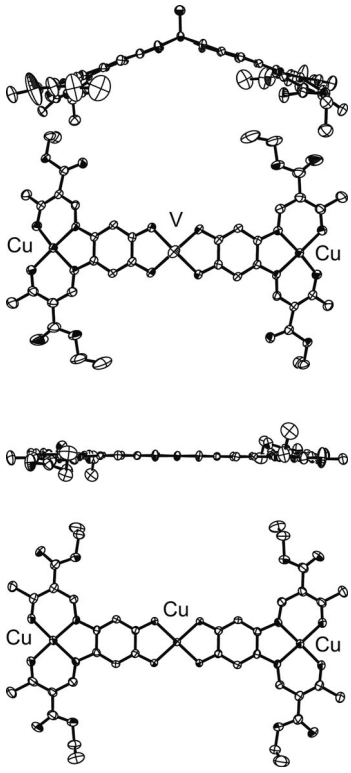

Figure 2. Top and side views of compound **1** (top) and **2** (bottom). Hydrogen atoms, counterions and additional solvent molecules are omitted for clarity. Thermal ellipsoids are shown at the 50% probability level.

lecular contacts were observed that could give rise to magnetic exchange interactions. The shortest intermolecular M–M distances are 6.00 Å for **1** (Cu–Cu) and 5.76 Å for **2** ($Cu_{N_2O_2}$–$Cu_{N_2O_2}$), which are shorter than the intramolecular distances; however, they were not considered to have a significant effect on the magnetic properties of the systems under investigation.

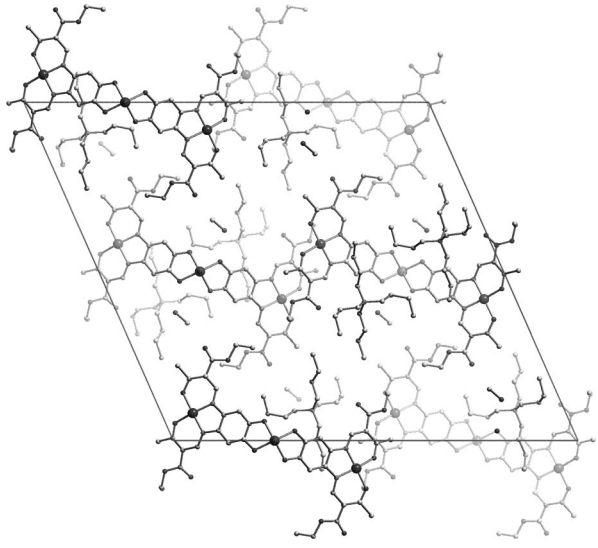

Figure 3. Packing of the molecules of **1** in the crystal.

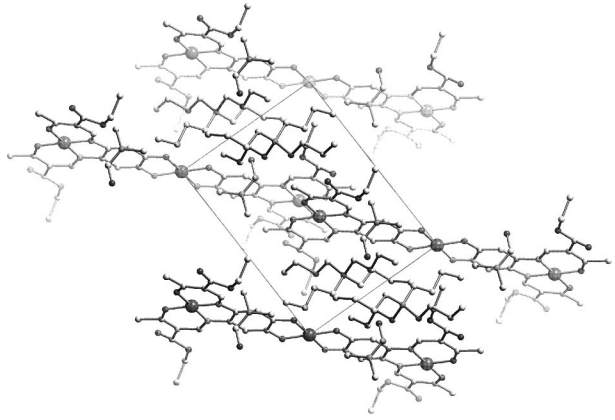

Figure 4. Packing of the molecules of **2** in the crystal.

Table 2. Selected intermolecular distances [Å] and angles [°] of **1**.

	D–H	H···A	A···D	D–H···A
O10–H10A···O4	0.84	1.92	2.74	168

Magnetic Susceptibility Data

Magnetic susceptibility measurements were performed in the temperature range from 300 to 2 K for both complexes by using a Quantum design MPMSR2-SQUID magnetometer. Figure 5 displays the thermal dependence of the $\chi_M T$ product (with χ_M being the molar susceptibility and T the temperature) at 0.05 T for both compounds. For both complexes, the room-temperature value is 1.24 and 1.31 cm^3 K/mol for **1** and **2**, respectively, which is close to the expected one for three noninteracting S = 1/2 centres (1.11 cm^3 K/mol for g = 2). The value for the trinuclear copper complex is slightly higher probably due to a higher g value of the central copper atom. Upon cooling, the $\chi_M T$ product remains almost constant in the case of **1** until below 25 K when an abrupt increase to a value of 1.52 cm^3 K/mol at 2 K was observed. In contrast to this, in the case of **2** the $\chi_M T$ product first slowly decreases upon cooling and below 100 K it decreases more rapidly. Below 10 K, a plateau is reached with $\chi_M T$ = 0.41 cm^3 K/mol, a value typical for one unpaired electron. This behaviour is an indication for ferromagnetic exchange interactions in the case of **1** and antiferromagnetic exchange interactions in the case of **2**.

The data were analysed assuming three linear aligned interacting S = 1/2 spin centres with the Hamiltonian given as:[1,13]

$$H = -J(S_{A1}S_B + S_{A2}S_B) - J'S_{A1}S_{A2}$$

where the local spins are denoted S_{A1}, S_{A2} and S_B with J and J' being the interaction parameters. The resulting expression for the magnetic susceptibility is given in the literature.[1,13] The influence of J' on the magnetic properties was assumed to be negligible, and a good agreement between the calculated and experimental data was obtained by imposing J' = 0. The used parameters for the two complexes are given in Table 3.

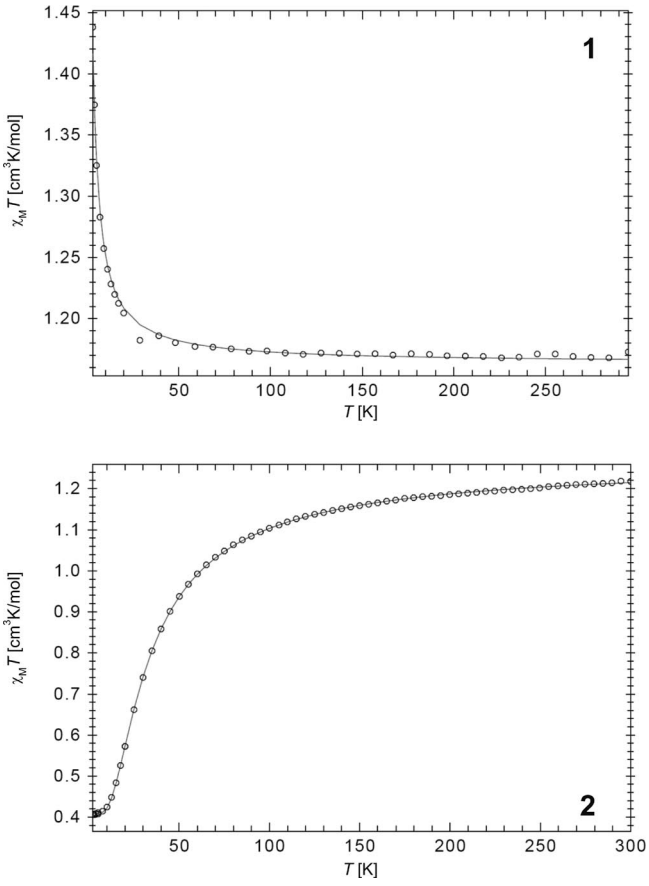

Figure 5. Plots of $\chi_M T$ product (open circles) vs. T for compounds **1** and **2** at 0.05 T. The solid lines represent the calculated temperature dependence with the model described in the text.

Table 3. Calculated parameters for the magnetic susceptibility by using the Hamiltonian above with a full-matrix diagonalisation.[15]

	J [cm^{-1}]	$g(Cu_{N_2O_2})$	g(V/Cu)	TIP
1	0.844	2.097	1.900	260.0×10^{-6}
2	–13.059	2.106	2.158	312.3×10^{-6}

The observed magnetic properties can be easily explained if the symmetry of the magnetic orbitals is considered, as illustrated in Scheme 2. In the case of **2**, all three copper centres are in a square-planar coordination sphere, and thus, the unpaired electron is located in the $d_{x^2-y^2}$ orbital. Those orbitals overlap with the σ-bonds of the bridging ligand, leading to antiferromagnetic interactions that can be explained with the super exchange mechanism. In contrast to this for **1**, the unpaired electron of the vanadyl ion is located in the d_{xy} orbital (square-pyramidal coordination sphere with the axial oxido group being the strongest ligand). As a consequence, the magnetic orbital of the vanadyl centre is rotated by 45° relative to the central copper centre and thus antiferromagnetic exchange interactions as described above are no longer possible. The magnetic orbitals of the copper and the vanadyl centre are orthogonal, and this strict orthogonality of the magnetic orbitals leads to ferromagnetic exchange interactions.

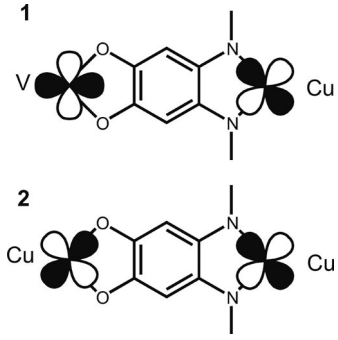

Scheme 2. Schematic representation of the orientation of the magnetic orbitals in **1** and **2**.

Conclusions

The two trinuclear complexes described in this article are further examples of how the concept of strict orthogonality of the magnetic orbitals can be used to obtain ferromagnetic exchange interactions. The same strategy used by O. Kahn et al. on dinuclear complexes can be transferred to trinuclear systems. One disadvantage of the ligand system used in this work is the relatively long exchange pathway that results in comparatively weak exchange interactions (J = +0.84 cm^{-1} and J = –13.06 cm^{-1} for **1** and **2**, respectively, in contrast to J = +118 cm^{-1} and J = –650 cm^{-1} for the dinuclear complexes by Kahn et al.[12]). However, the usefulness of this ligand system lies in its flexibility with regard to the coordinated metal centres. We could already demonstrate that the ligands are also suitable for the synthesis of iron(II) spin-crossover complexes.[10] The next step will be to prepare trinuclear complexes with two (or even more) iron(II) spin-crossover sites linked by different metal centres and to investigate their magnetic properties.

Experimental Section

Synthesis: All syntheses were carried out under an atmosphere of argon by using Schlenk tube techniques. All solvents were purified as described in the literature[14] and distilled under an atmosphere of argon. The synthesis of H_4L is described in literature.[9]

[H_2CuL]: A suspension of H_4L (1.05 g, 2.5 mmol) and copper acetate monohydrate (0.5 g, 2.5 mmol) in methanol (35 mL) was heated at reflux for 1 h. After cooling, the light-brown precipitate was filtered off, washed with ethanol (2 × 10 mL) and dried in vacuo. Yield: 1.20 g (99%). $C_{20}H_{22}CuN_2O_8$ (481.94): calcd. C 49.84, N 5.81, H 4.60; found C 49.11, N 5.71, H 4.59. MS (DEI+): m/z (%) = 481.1 (100) [CuL]$^+$, 393.1 (46) [CuL – 2OEt]$^+$, 347.1 (64) [CuL – OEt – COOEt – OH]$^+$. IR (nujol): $\tilde{\nu}$ = 1718 (C=O, COOEt), 1669 (C=O, COMe), 3555 (s, OH), 3406 (br., OH) cm^{-1}.

[V(O)Cu_2L_2](N*n*Bu_4)$_2$·2MeOH: To a solution of [H_2CuL] (0.59 g, 1.2 mmol) in DMF (20 mL) was added a solution of TBAH (1 M in methanol, 2.5 mL, 2.5 mmol), and the solution was stirred at

room temperature for 30 min. After this time, a solution of vanadyl acetylacetonate (0.19 g, 0.74 mmol) in methanol (15 mL) was added to the solution, and the mixture was stirred for 20 min. After this time, any formed precipitate was filtered off, and the solution was layered with ethyl ether (160 mL). After one week, dark-brown crystals were formed that were filtered off and dried in vacuo. Yield: 0.53 g (27%). $C_{74}H_{120}Cu_2N_6O_{19}V$ (1575.81): calcd. C 56.40, H 7.68, N 5.33; found C 56.08, H 7.70, N 5.38. MS (FAB–): *m*/*z* (%) = 1026 (100) $[Cu_2VL_2]^-$, 1268 (40) $[Cu_2VL_2N\textit{n}Bu_4]^-$, 562 (70) $[CuLVO_2]^-$. MS (FAB+): *m*/*z* (%) = 242 (100) $[N\textit{n}Bu_4]^+$. IR (nujol): $\tilde{\nu}$ = 1683 (C=O, COOEt), 1663 (C=O, COMe) cm^{-1}.

$[Cu_3L_2]\{N(\textit{n}Bu)_4\}_2\cdot 2DMF$: To a solution of $[H_2CuL]$ (0.55 g, 1.1 mmol) in DMF (15 mL) was added a solution of TBAH (1 M in methanol, 2.5 mL, 2.5 mmol), and the solution was stirred at room temperature for 30 min. After this time, a solution of copper acetylacetonate (0.16 g, 0.61 mmol) in methanol (20 mL) was added, and the mixture was stirred for 20 min. After this time, any formed precipitate was filtered off, and the solution was layered with ethyl ether (160 mL). After one week, dark-red crystals were formed that were filtered off and dried in vacuo. Yield: 0.72 g (38%). $C_{78}H_{126}Cu_3N_8O_{18}$ (1654.52): calcd. C 56.22, H 7.68, N 6.77; found C 56.23, H 7.70, N 6.59. MS (FAB–): *m*/*z* (%) = 1023 (70) $[Cu_3L_2]^-$, 1265 (30) $[Cu_3L_2N\textit{n}Bu_4]^-$, 479 (60) $[CuL]^-$. MS (FAB+): *m*/*z* (%) = 242 (100) $[N\textit{n}Bu_4]^+$. IR (nujol): $\tilde{\nu}$ = 1683 (C=O, COOEt), 1665 (C=O, COMe) cm^{-1}.

Magnetic Measurements: Magnetic measurements of the fine crystalline samples were performed with a Quantum-Design-MPMSR2-SQUID-Magnetometer in a temperature range from 2 to 300 K. The measurements were carried out at 0.05 T in the settle mode. The data were corrected for the magnetisation of the sample holder and diamagnetic corrections were made by using tabulated Pascal's constants.

X-ray Crystallography: The intensity data of **1** were collected with a Nonius KappaCCD diffractometer by using graphite-monochromated Mo-K_α radiation. The intensity data of **2** were collected with an Oxford XCalibur diffractometer by using graphite-monochromated Mo-K_α radiation. Data were corrected for Lorentz and polarisation effects. The structure was solved by direct methods (SIR97[16]) and refined by full-matrix least-square techniques against F_0^2 (SHELXL-97[17]). The hydrogen atoms were included at calculated positions with fixed thermal parameters. ORTEP-III was used for structure representation.[18] Crystallographic data are summarised in Table 4. Selected distances and angles are presented in Table 1. CCDC-744751 (for **1**) and -744752 (for **2**) contain the supplementary crystallographic data for this paper. These data can be obtained free of charge from The Cambridge Crystallographic Data Centre via www.ccdc.cam.ac.uk/data_request/cif.

Table 4. Crystallographic data of the trinuclear complexes discussed in this work.

Complex	**1**	**2**
Empirical formula	$C_{74}H_{120}Cu_2N_6O_{19}V$	$C_{78}H_{126}Cu_3N_8O_{18}$
Formula weight	1575.81	1654.52
Temperature [K]	200	200
Crystal size [mm]	0.32 × 0.10 × 0.09	0.50 × 0.41 × 0.11
Crystal system	monoclinic	triclinic
Space group	*C*2/*c*	$P\bar{1}$
λ [Å]	0.71073	0.71073
a [Å]	31.680(4)	10.157(2)
b [Å]	8.2730(1)	14.062(4)
c [Å]	34.2020(5)	10.356(8)
α [°]	90	66.90(4)
β [°]	113.8920(7)	73.66(3)
γ [°]	90	86.38(2)
V [Å^3]	8063.38(18)	2059.0(14)
Z	4	1
$\rho_{calcd.}$ [g/cm^3]	1.298	1.334
μ [1/mm]	0.705	0.838
F(000)	3356.0	881.0
Θ range [°]	3.134–27.485	3.7723–24.9996
Index ranges	–40/40	–12/12
	–10/10	–16/16
	–44/44	–19/19
Reflections collected	70232	27148
Reflections unique	9228	7267
Data/restrains/parameters	9228/0/470	7267/0/499
R_1 (all)	0.0494 (0.0778)	0.0397 (0.0751)
wR_2	0.1223 (0.1364)	0.1016 (0.1237)
GooF	1.038	1.051

Acknowledgments

This work has been supported financially by the Deutsche Forschungsgemeinschaft (SPP 1137) the Fonds der Chemischen Industrie, the Center for Integrated Protein Science Munich (CIPSM) and the University of Munich. The authors thank P. Mayer for acquisition of the crystallographic data of **1**.

[1] O. Kahn, *Molecular Magnetism*, Wiley VCH, Weinheim, **1993**.
[2] O. Kahn, *Inorg. Chim. Acta* **1982**, *62*, 3–14.
[3] a) P. W. Anderson, H. Hasegawa, *Phys. Rev.* **1955**, *100*, 675–681; b) G. Blondin, J.-J. Girerd, *Chem. Rev.* **1990**, *90*, 1359–1376; c) T. Glaser, T. Beissel, E. Bill, T. Weyhermüller, V. Schünemann, W. Meyer-Klaucke, A. X. Trautwein, K. Wieghardt, *J. Am. Chem. Soc.* **1999**, *121*, 2193–2208.
[4] a) H. C. Longuet-Higgins, *J. Chem. Phys.* **1950**, *18*, 265–274; b) H. Iwamura, *Adv. Phys. Org. Chem.* **1990**, *26*, 179–253.
[5] a) B. Weber, *Coord. Chem. Rev.* **2009**, *253*, 2432–2449; b) B. Weber, E.-G. Jäger, *Eur. J. Inorg. Chem.* **2009**, 465–477.
[6] a) B. Weber, E. Kaps, J. Weigand, C. Carbonera, J.-F. Letard, K. Achterhold, F.-G. Parak, *Inorg. Chem.* **2008**, *47*, 487–496; b) B. Weber, E. S. Kaps, J. Obel, W. Bauer, *Z. Anorg. Allg. Chem.* **2008**, 1421–1426; c) B. Weber, C. Carbonera, C. Desplanches, J.-F. Létard, *Eur. J. Inorg. Chem.* **2008**, 1589–1598; d) B. Weber, E. S. Kaps, C. Desplanches, J.-F. Létard, K. Achterhold, F.-G. Parak, *Eur. J. Inorg. Chem.* **2008**, 4891–4898; e) W. Bauer, B. Weber, *Inorg. Chim. Acta* **2009**, *362*, 2341–2346; f) B. Weber, E. Kaps, *Heteroat. Chem.* **2005**, *16*, 391–397; g) B. Weber, F.-A. Walker, *Inorg. Chem.* **2007**, *46*, 6794–6803; h) B. Weber, E. S. Kaps, J. Obel, K. Achterhold, F. G. Parak, *Inorg. Chem.* **2008**, *47*, 10779–10787; i) B. Weber, R. Tandon, D. Himsl, *Z. Anorg. Allg. Chem.* **2007**, *633*, 1159–1162; j) B. Weber, E. S. Kaps, C. Desplanches, J.-F. Létard, *Eur. J. Inorg. Chem.* **2008**, 2963–2966.
[7] a) B. R. Müller, G. Leibeling, E.-G. Jäger, *Chem. Phys. Lett.* **2000**, *319*, 368–374; b) B. Weber, E.-G. Jäger, *Z. Anorg. Allg. Chem.* **2009**, *635*, 130–133.
[8] B. Weber, W. Bauer, J. Obel, *Angew. Chem.* **2008**, *120*, 10252–10255; *Angew. Chem. Int. Ed.* **2008**, *47*, 10098–10101.
[9] B. Weber, J. Obel, *Z. Anorg. Allg. Chem.*, DOI: 10.1002/zaac.200900241.
[10] a) B. Weber, J. Obel, D. Henner-Vasquez, W. Bauer, *Eur. J. Inorg. Chem.*, **2009**, 5527–5534, preceding paper; b) D. Henner-Vasquez, Report, University of Munich.
[11] D. T. Rosa, R. A. Reynolds, S. M. Malinak, D. Coucouvanis, *Inorg. Synth.* **2002**, *33*, 112–119.

[12] O. Kahn, J. Galy, Y. Journaux, J. Jaud, I. Morgenstern-Badarau, *J. Am. Chem. Soc.* **1982**, *104*, 2165–2176.
[13] R. Veit, J.-J. Girerd, O. Kahn, F. Robert, Y. Jeannin, *Inorg. Chem.* **1986**, *25*, 4175–4180.
[14] Autorenkollektiv: *Organikum*, Johann Ambrosius Barth Verlagsgesellschaft mbH **1993**.
[15] Simulation of the experimental magnetic data with a full-matrix diagonalisation of exchange coupling was performed with the julX program developed by E. Bill/Max-Planck-Institute for Bioinorganic Chemistry.
[16] *SIR97*, Campus Universitario Bari, **1997**: A. Altomare, M. C. Burla, G. M. Camalli, G. Cascarano, C. Giacovazzo, A. Guagliardi, A. G. G. Moliterni, G. Polidori, R. Spagna, *J. Appl. Crystallogr.* **1999**, *32*, 115.
[17] G. M. Sheldrick, *SHELXL97*, University of Göttingen, Germany, **1993**.
[18] C. K. Johnson, M. N. Burnett, *ORTEP-III*, Oak-Ridge National Laboratory, Oak-Ridge, **1996**; L. J. Farrugia, *J. Appl. Crystallogr.* **1997**, *30*, 565.

Received: August 27, 2009
Published Online: November 4, 2009

